Anisotropies in the diffuse gamma-ray background measured by the Fermi-LAT

A. Cuoco[a], T. Linden[b], M.N. Mazziotta[c], J.M. Siegal-Gaskins[d], Vincenzo Vitale[e,*], for the Fermi-LAT Collab.,
E.Komatsu[f]

[a]*Stockholm University - Oskar Klein Center AlbaNova University Center, Fysikum, SE-10691, Stockholm, Sweden*
[b]*Department of Physics, University of California, Santa Cruz, 1156 High Street, Santa Cruz, CA, 95064*
[c]*Istituto Nazionale di Fisica Nucleare, Sezione di Bari, 70126 Bari, Italy*
[d]*Einstein Postdoctoral Fellow, California Institute of Technology 1200 E. California Blvd., Pasadena, CA 91125*
[e]*Istituto Nazionale di Fisica Nucleare, Sezione di Tor Vergata, 00133 Roma, Italy*
[f]*Texas Cosmology Center and Department of Astronomy, Univ. of Texas, Austin, Dept. of Astronomy, 2511 Speedway, Austin, TX 78712*

Abstract

The small angular scale fluctuations of the (on large scale) isotropic gamma-ray background (IGRB) carry information about the presence of unresolved source classes. A guaranteed contribution to the IGRB is expected from the unresolved gamma-ray AGN while other extragalactic sources, Galactic gamma-ray source populations and dark matter Galactic and extragalactic structures (and sub-structures) are candidate contributors.

The IGRB was measured with unprecedented precision by the Large Area Telescope (LAT) on-board of the Fermi gamma-ray observatory, and these data were used for measuring the IGRB angular power spectrum (APS). Detailed Monte Carlo simulations of Fermi-LAT all-sky observations were performed to provide a reference against which to compare the results obtained for the real data set. The Monte Carlo simulations are also a method for performing those detailed studies of the APS contributions of single source populations, which are required in order to identify the actual IGRB contributors.

We present preliminary results of an anisotropy search in the IGRB. At angular scales $<2°$ (e.g. above multipole 155), angular power above the photon noise level is detected, at energies between 1 and 10 GeV in each energy bin, with statistical significance between 7.2 and 4.1σ. The energy not dependence of the fluctuation anisotropy is pointing to the presence of one or more unclustered source populations, while the energy dependence of the intensity anisotropy is consistent with source populations having average photon index $\Gamma = 2.40\pm0.07$.

Keywords:

1. IGRB Anisotropy

In all-sky high-energy gamma-ray observations an intense diffuse emission originating from the Milky Way is visible. Above 30 MeV the large majority of this emission is produced by cosmic-ray (CR) ions interacting with the Galactic interstellar gas via neutral pion production and decay, and inverse Compton (IC) scattering of interstellar radiation fields photons off CR electrons. A fainter, almost isotropic on large angular scales, gamma-ray background (IGRB) has also been detected, first by the SAS-2 mission [1]. Later the IGRB energy spectrum was measured with good accuracy by the Energetic Gamma-Ray Experiment Telescope [2],[3] on-board the Compton Observatory and recently with the LAT detector on-board the Fermi gamma-ray observatory [4].

A considerable part of the IGRB has likely extragalactic origin (EGB) and carries information about the non-thermal phenomena in the universe. The IGRB has a guar-anted contribution from the known extragalactic gamma-ray sources. AGN represent the largest source population above 30 MeV detected by EGRET [5] and the LAT detector [6],[7]. Therefore, undetected AGN (those below the current detection threshold) are the most likely candidates for the origin of the bulk of the EGB emission. The estimates of the EGB fraction originating from AGN vary from 20 and $\approx$100% depending on the energy and the model (see [8] and references therein). Another main extragalactic candidate is star-burst galaxies [9]. A fraction of the IGRB might also originate from the sum of Galactic nearby sources such as millisecond pulsars (MSPs) [10].

The IGRB anisotropy study provides us also with a method for the indirect search for dark matter (DM) with gamma rays, which is very complementary to the study of the main DM overdensities, such as the Galactic center [11] and dwarf spheroidal galaxies [12] and also complementary to the search of lines [13] or other spectral features from large areas of the sky. In fact the sub-structures of the Milky Way dark matter halo and the dark matter halos in the local universe might produce an imprint in the

IGRB. Dark matter overdensities might shine in gamma rays both in the case of pair-annihilating DM particles (with the resulting gamma-ray flux proportional to the square of the dark matter density) and pseudo-stable decaying ones (with flux proportional to the density). The largest substructures of the Galactic halo might be individually detectable while the majority of them are likely to be under detection threshold but still be able to contribute to the IGRB [14] and also induce small scale anisotropies [15].

Information on the IGRB origins is carried by its small scale angular fluctuations. If a diffuse emission originates from unresolved source populations then small angular scale fluctuations will arise because of the variation of number density of the sources in different sky directions. These fluctuations are a feature of the source distribution and will persist also in the limit of infinite statistics, contrary to Poisson fluctuations (photon noise) which decreases with increasing event statistics. It is therefore possible to discriminate between sources induced anisotropies and photon noise, if one is provided with a sufficient data statistics. One method for the study of the IGRB anisotropy is the APS measurement. In theoretical studies of the IGRB anisotropy the following contributors were considered: (a) blazars [17],[18],[19]; (b) star-forming galaxies [20]; (c) Galactic MSPs [21]; (d) annihilating or decaying dark matter in Galactic sub-halos [22],[23],[24]; (e) dark matter in extragalactic structures [16],[17],[19],[24],[25] and [26],[27], [28],[29]. In these studies it is also shown that intrinsic clustering of many populations candidates has a sub-dominant effect on the angular power spectrum in multipole range between 100-500.

Here we report on a search for anisotropies in the IGRB, performed with the data taken with the LAT detector onboard of the Fermi satellite.

2. The LAT and the Data Analysis

The Fermi Large Area Telescope has a wide field of view (2.4 sr) and a large effective area ($\approx$8000 cm^2 for normally-incident photons above 1 GeV). LAT is a pair-conversion telescope with a modular structure made of 4$\times$4 *towers*. Each tower is composed by: (i) a precision silicon tracker (18 planes of Si-strip detectors coupled with W conversion planes, with a total of 1.5 X$_0$ for the normal incidence. The Si tracker is made of a first thinner segment, called front, with a better angular resolution and a second thicker one, called back); (ii) a CsI homogeneous calorimeter (8.5 X$_0$ for the normal incidence). The pair-conversion telescope is covered with an anti-coincidence detector that allows for rejection of charged particle events. Full details of the instrument, including technical information about the detector, on-board and ground data processing, and mission-oriented support, are given in [31].

Data taken during the first 56.6Ms of observation ($\approx$22 months) were used. The experimental data and simulations were analyzed with the LAT analysis software Science Tools version v9r15p4 with P6_V3 LAT instrument response functions (IRFs).

The main analysis steps were:

- Data Preparation. By means of the gtselect tool: (i) events of *diffuse* class were selected and with energy between 1 and 50 GeV; (ii) data with zenith angle exceeding 105° were rejected to reduce Earth gamma-ray albedo contamination; (iii) events converted in the front and back tracker segments have also been divided in order to be analyzed separately. Periods in which with LAT was in the South Atlantic Anomaly, not in survey mode or with rocking angle exceeding 52° were discarded with the tool gtmktime. The integrated livetime was calculated using the gtltcube tool (photon injection step size $\cos(\theta) = 0.025$, pixel size of 0.125° corresponding to a HEALPix [30] map with Nside = 512 resolution)

- Exposure. Exposure maps were calculated using the gtexpcube tool with the same pixel size as for gtltcube, for 42 logarithmic energy bins spanning 1.04 to 50 GeV, in order to have a good knowledge of the energy dependence of the exposure.

  The *event shuffling technique* is an alternative method for the exposure calculation that does not rely on the Monte Carlo based calculation of the exposure implemented in the Science Tools. It was used for cross-checking possible exposure systematic errors. With this method the arrival directions of pairs of detected events are swapped in the instrument coordinates, this produces anexposure map wih arbitrary normalization. The same technique has also been used to search for anisotropy in the CR electrons arrival directions, measured with the LAT, in [34].

- Intensity Maps. Counts maps were built with the selected data. Both the photon counts and exposure maps were converted into HEALPix-format maps with Nside = 512, and HEALPix gamma-ray intensity maps in four energy bins were obtained.

- Map Masking. Regions of the sky heavily contaminated by Galactic diffuse emission were excluded by masking Galactic latitudes $|b| < 30°$, and masking sources in the Fermi 11-month catalog [6] within a 2° angular radius. In this study we focused on multipoles $l \gtrsim 150$ (corresponding to angular scales < 2°), since lower multipoles (corresponding to correlations over larger angular scales) are likely more contaminated by Galactic diffuse emission.

- Intensity and Fluctuation APS. The angular power spectra were calculated for the intensity map I(ψ), where ψ is the sky direction. The angular power spectrum is given by the coefficients $C_l = < |a_{lm}|^2 >$ with the a_{lm} determined by expanding the map in

2

spherical harmonics. The intensity APS indicates the dimensionful amplitude of the anisotropy and can be compared with predictions for source classes whose collective intensity is known or assumed. A dimensionless fluctuation APS has also been calculated by dividing the intensity APS spectrum C_l of a map by the mean sky intensity (outside of the mask) squared $<I>^2$. In the case of the shuffling technique only the intensity fluctuation APS can be obtained. The angular power spectra of the maps were calculated using the HEALPix package [30]. The measured APS were corrected for the power suppression due to the beam and pixel window functions, and an approximate correction, valid at multipoles $l > 100$, was applied to account for the reduction in angular power due to masking. For each energy bin, the APS of the maps of front- and back-converting events were calculated separately and then combined by weighted average.

- Validation Studies. Careful checks of the procedures and the related parameters were performed as well as tests for assessing the origin of the measured angular power. The full analysis was applied to a simulated point source population, in order to compare the APS determined with the analysis chain and the one which could be analytically calculated. The dependence of the results on the instrument response functions (IRFs), as also on the masking have also been studied. For the latter in particular both the latitude cut with which the Galactic plane was excluded and the radius of the circle with which each know source was masked, were varied. In order to further evaluate the effect of residual Galactic diffuse emission on the APS the analysis was repeated on the data after the subtraction of a model of the Galactic diffuse emission (*Galactic Foreground Cleaning*). The details of these studies will be given in the final publication of the anisotropy study.

3. Simulated Models

Detailed Monte Carlo simulations of Fermi-LAT all-sky observations were performed. The purpose was to have a reference model to be compared with the real data set. The status-of-art of the LAT modelling was used by means of the gtobssim tool. This code required as an input a detailed spatial and spectral model of the emission to be simulated. Details of real LAT observations, such as spacecraft pointing and live-time history, can be also included in the simulations. The gtobssim tool generates simulated photon events. The P6_V3_DIFFUSE IRFs and the actual spacecraft pointing and live-time history matching the observational time interval of the data were used to generate the simulated data sets. Two models of the gamma-ray sky were simulated. Each model is the sum of three components:
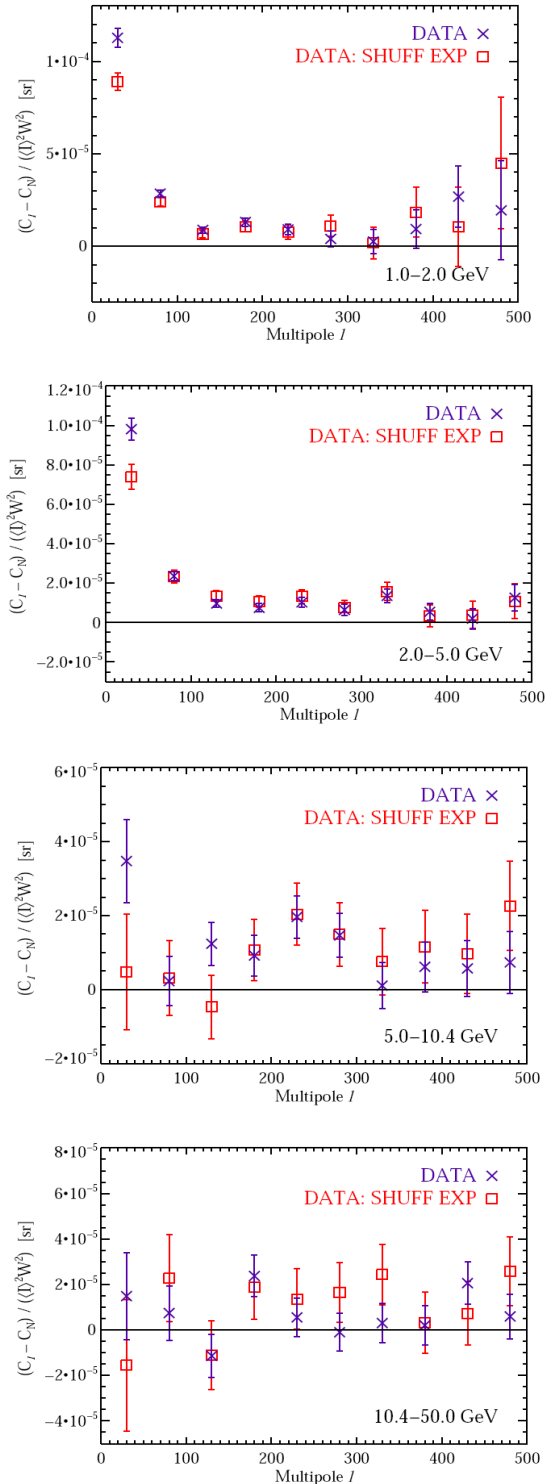

Figure 1: PRELIMINARY. Fluctuation APS of the IGRB minus photon noise, in four energy bins. For isotropic emission this difference would be consistent with zero. The large angular power at $l < 155$ is likely originating from Galactic diffuse emission. For $l > 155$ the measured power excess is approximately constant in multipole, suggesting that it originates from one or more unclustered source populations. The APS obtained with the event shuffling technique are also reported. The two different methods provide consistent results and show that possible inaccuracies in the exposure calculation have a negligible impact on these results.
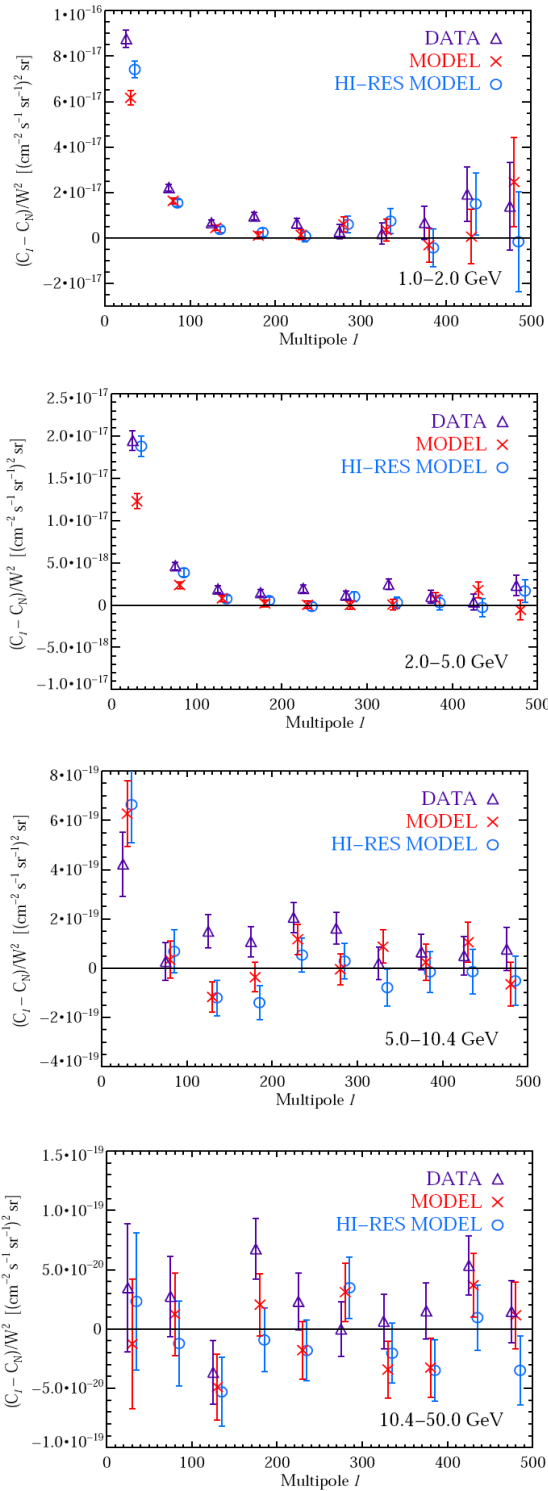
3

Figure 2: PRELIMINARY. Intensity APS of the IGRB minus photon noise, in four energy bins. APS of the experimental data, simulated default model and high resolution models are reported. The measured power above l ≈ 155 is not found in either of the two models. Points from different data sets are offset slightly in multipole for clarity.
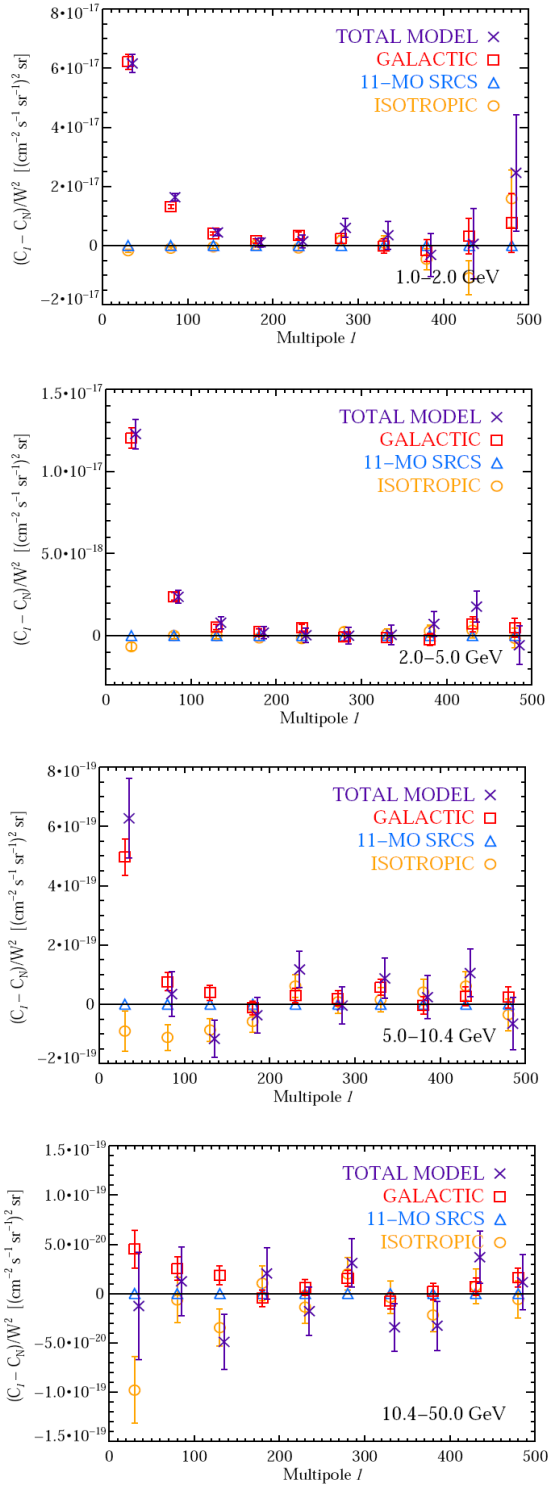

Figure 3: PRELIMINARY. Intensity APS of the IGRB minus photon noise, in four energy bins. The APS of the single model components are reported. The large power in the models at $l < 155$ is due to the GAL component. The isotropic component (ISO) provides APS compatible with zero as expected for isotropic emission; likewise, the source component (CAT) provides no contribution because all sources were effectively masked. Total Model points are offset slightly in multipole for clarity.

1. GAL - a model of the Galactic diffuse emission;
2. CAT - the 1451 sources in the first Fermi-LAT source catalog (1FGL) [6];
3. ISO - an isotropic background.

The same CAT and ISO components are included in both models. These differ only for the model for the GAL component in use. GAL describes both the spatial distribution and the energy spectrum of the Galactic diffuse emission. The GAL component for the reference sky model used in this analysis (hereafter, Model) is the recommended Galactic diffuse model for LAT data analysis, gll_iem_v02.fit [32], which has an angular resolution of $0.5°$. This model was used to obtain the 1FGL catalog; a detailed description can be found in [33].

An higher-resolution model (Hi-Res Model) was simulated for comparison, so that was possible to test impact of smaller details in the Galactic diffuse emission. This model (ring_21month_v1.fit) is internal to the LAT collaboration, and was built using the same method as gll_iem_v02.fit, but differs primarily in the following ways: (i) this model was constructed using 21 months of Fermi-LAT observations, while gll_iem_v02.fit was based on 9 months of data; (ii) the grid angular resolution for this model is $0.125°$, in order fully exploit the angular resolution of the CO maps [35] used to build it; and (iii) additional large-scale structures, such as the Fermi bubbles [36], are included in the model through the use of simple templates.

The single power law spectrum is assumed for all the sources in CAT and the locations, average integral fluxes, and photon spectral indices are as reported in the 1FGL catalog. All 1451 sources were included in the simulation. ISO represents the sum of the Fermi-measured IGRB and an additional isotropic component presumably due to un-rejected charged particles; for this component the spectrum template isotropic_iem_v02.txt was used. For both the Model and the Hi-Res Model, the sum of the three simulated components results in a description of the gamma-ray sky that closely approximates the angular-dependent flux and energy spectrum of the all-sky emission measured by the Fermi-LAT. Although the simulated models may not accurately reproduce some large-scale structures, e.g., Loop I [37] and the Fermi bubbles [36], these features are not expected to induce anisotropies on the small angular scales on which we focus in this work.

The simulated models were processed and their angular power spectra calculated using the same analysis pipeline as the data. In Figure 2 the APS of the data and models are shown. The contributions to APS of the individual components of the default model are shown in Figure 3. At all energies the only component of the models contributing significantly to $l < 155$ is the Galactic diffuse emission. The contribution from the isotropic component is negligible, since this component is isotropic by construction and thus, after the photon noise is subtracted, it should only contribute to the monopole ($l=0$) term. The source catalog component contributes zero power at all energies and multipoles because all these sources were effectively masked, giving rise to a negligible residual effect. We remark that in general the APS of distinct components are not linearly additive due to contributions from cross-correlations between the components.

4. Results

Significant ($>3\sigma$ CL in each energy bin) angular power above the photon noise level (see Figure 1) is detected in the data at multipoles $155 \leq l \leq 504$ for energies below 10 GeV, and at lower significance in the 10-50 GeV energy bin. The sensitivity of the measurement at high energies is limited by the small statistics. The measured angular power is consistent with a constant value within each energy bin, which suggests that it originates from one or more unclustered populations of point sources. The fluctuation angular power detected in this analysis falls below the level predicted for some models of blazars, MSPs, and Galactic and extragalactic DM structures, and so the measured amplitude of the fluctuation angular power can limit the contribution to the total IGRB intensity of each source class. The measured fluctuation angular power is almost independent of energy, and so it might originate from a single dominant source class, although a mild energy dependence cannot be excluded.

The energy dependence of the intensity angular power of the data is well-described by that arising from a single source class with a power-law energy spectrum with photon index $\Gamma = 2.40 \pm 0.07$. This value is compatible with the mean intrinsic spectral index for blazars as determined from recent Fermi-LAT measurements.

The study of the currently available Fermi-LAT data has provided us with the first detection of small scale-angular power in the IGRB. Future analyses on larger data sets could allow anisotropy searches to be extended to higher energies, and will likely be more sensitive to features in the anisotropy energy spectrum.

Detailed studies of population models are required in order to: (i) identify the source classes which are actually contributing to the IGRB anisotropy and (ii) provide upper-limits to the contribution of other candidate source populations. A possible approach is the study of the APS induced by source population models and the following Monte Carlo simulation of the model emission, with the best possible characterization of the instrument response.

For an example, in the DM case a model of all its distribution structures and sub-structure (Galactic and in the local Universe) which can provide contribution should be considered [38], and furthermore a given particle physics model should be assumed, or at least the DM particle mass and the annihilation cross-section for self-annihilating DM, or the mean life-time for pseudo-stable decaying DM. Then the APS induced by these DM models can be obtained with the same procedure which was used for the simulated Model and Hi-Res Model of section 3.

References

[1] Fichtel, C. E., et al. 1975, ApJ, 198, 163
[2] Sreekumar, P., et al. 1998, ApJ, 494, 523
[3] Strong, A. W., Moskalenko, I. V., & Reimer, O. 2004, ApJ, 613, 956
[4] A. Abdo et al. (Fermi-LAT Collab.), 2010 Phys.Rev.Lett. 104, 101101
[5] R.C. Hartman et al. 1999, ApJS, 123, 79
[6] A.Abdo et al. (Fermi-LAT Collab.) 2010 ApJS 188 405A
[7] aXiv:1108.1435 (Fermi-LAT Collab.), submitted to ApJS
[8] A.Abdo et al (Fermi-LAT Collab.), 2010 ApJS 720 435
[9] B. D. Fields, V. Pavlidou, and T. Prodanovic, 2010 ApJ 722, L199
[10] C.-A. Faucher-Giguere and A. Loeb 2010 JCAP 1001, 005
[11] V.Vitale and A. Morselli for the Fermi-LAT collab. 2009 arXiv0912.3828V
[12] M. Ackermann, et al (Fermi-LAT Collab.), 2011 arXiv1108.3546T
[13] A. Abdo et al. (Fermi-LAT Collab.) 2010 PhRvL. 104i1302A
[14] Ullio et al 2002 PhRvD 66l3502
[15] Siegal-Gaskins, J. M. 2008 JCAP 0810 040
[16] S. Ando and E. Komatsu, 2006 Phys.Rev.D73, 023521 (2006)
[17] S. Ando, et al, 2007 Phys.Rev. D75, 063519
[18] S. Ando, et al, 2007 MNRAS 376, 1635 (2007)
[19] F. Miniati, et al. 2007 ApJ. 667, L1
[20] S. Ando and V. Pavlidou, 2009 MNRAS 400, 2122
[21] J. M. Siegal-Gaskins, et al. 2011 MNRAS 415, 1074S
[22] J. M. Siegal-Gaskins, JCAP 0810, 040 (2008), 0807.1328.
[23] S. Ando, 2009 Phys.Rev. D80, 023520
[24] M. Fornasa, et al., 2009 Phys.Rev. D80, 023518
[25] A. Cuoco,et al. , 2008 Phys.Rev. D77, 123518
[26] L. Zhang and G. Sigl, 2008 JCAP 0809, 027
[27] M. Taoso, et al., 2009 Phys.Rev. D79, 043521
[28] A. Ibarra, D. Tran, and C. Weniger, 2010 Phys.Rev. D81,023529
[29] A. Cuoco, A. Sellerholm, J. Conrad, and S. Hannestad 2010, 1005.0843.
[30] K. Gorski, et al. 2005, ApJ. 622, 759
[31] W. Atwood et al. (Fermi-LAT Collab.) 2009 , ApJ. 697, 1071
[32] The default diffuse model used in this analysis as well as the isotropic spectral template are available from http://fermi.gsfc.nasa.gov/ssc/data/access/lat/BackgrounDModels.html
[33] http://fermi.gsfc.nasa.gov/ssc/data/access/lat/ring_for_FSSC_final4.pdf
[34] M. Ackermann, et al.(Fermi-LAT Collab.) 2010 Phys. Rev. D 82, 092003
[35] T. Dame, D. Hartmann, and P. Thaddeus, 2001 ApJ 547, 792.
[36] M. Su, T. R. Slatyer, and D. P. Finkbeiner, 2010 ApJ 724 1044
[37] J.-M. Casandjian and I. Grenier (Fermi-LAT Collabo.) 2009, arXiv:0912.3478.
[38] M. Fornasa, et al, 2011 these proceedings